Article

Highly Efficient Regioselective Acylation of Dihydromyricetin Catalyzed by Lipase in Nonaqueous Solvents

Song Zhu [1,2], **Baoshuang Du** [1,2], **Dejian Huang** [3], **Yongmei Xia** [1], **Shangwei Chen** [1] **and Yue Li** [1,4,*]

1 State Key Laboratory of Food Science and Technology, Jiangnan University, Wuxi 214122, China; zhusong@jiangnan.edu.cn (S.Z.); dbs199703@163.com (B.D.); ymxia@126.com (Y.X.); chenshangwei@jiangnan.edu.cn (S.C.)
2 International Joint Laboratory on Food Safety, Jiangnan University, Wuxi 214122, China
3 Department of Food Science and Technology, National University of Singapore, Singapore 117543, Singapore; fsthdj@nus.edu.sg
4 School of Food Science and Technology, Jiangnan University, Wuxi 214122, China
* Correspondence: liyue@jiangnan.edu.cn; Tel./Fax: +86-510-85197876

Abstract: This study aimed to explore the enzymatic acylation of dihydromyricetin (DHM) to synthesized DHM derivatives with a different substituted carbon chain to improve its liposolubility. In the presence of Lipozyme TL IM, DHM was butyrylated in a 96.28% conversion in methyl *tert*-butyl ether under the optimized conditions (molar ratio of DHM to vinyl butyrate, 1:20; lipase dosage, 0.4 U/mg DHM; temperature, 50 °C; stirrer speed, 200 rpm; reaction time, 72 h). Liquid chromatography-mass spectrometry (LC-MS) and nuclear magnetic resonance (NMR) spectroscopy revealed that two acylation products were formed; these were 7-*O*-acyl-DHM and 3-*O*-acyl-DHM. In addition, the liposolubility of the DHM derivatives increased with the increase in the substituted carbon chain length; their antioxidant activities were higher than that of DHM in the lecithin peroxidation system, and C8-DHM had a better effect. Therefore, enzymatic acylation broadens the application of DHM in a lipid system in the food field.

Keywords: dihydromyricetin; acylation; Lipozyme TL IM; conversion; lecithin peroxidation

1. Introduction

Dihydromyricetin (DHM), also known as ampelopsin, is a natural aglycone flavonoid that is primarily extracted from *Ampelopsis grossedentata* [1]. *Ampelopsis grossedentata* is distributed in southern China and its leaves have been used in teas (Teng cha) and herbal medicines to treat coughs, fever, and sore throats for hundreds of years. It contains over 30% DHM [2,3]. DHM performs many biological functions, including exhibiting antioxidant, anti-tumor, anti-bacterial, and anti-inflammatory activities [4], regulating glucose metabolism and protecting the liver. Because of these activities, DHM has received considerable attention. However, its low liposolubility and bioavailability limit its application in pharmaceuticals, foods, cosmetics, and other fields. Many studies have reported that acylation can improve the liposolubility of flavonoids [5,6]. Acylation can be classified into chemical and enzymatic acylation. Compared with chemical acylation, enzymatic acylation has higher regioselective, mild reaction conditions and can be completed in a single step; hence, it has a wider application scope [7,8]. At present, the majority of studies into the enzymatic acylation of flavonoids have focused on glycosylated flavonoids, with only a few studies being available in the context of aglycone flavonoids, especially those based on DHM.

The activities of flavonoids are closely related to their structure; therefore, the presence of flavonoid acylation sites is particularly critical, especially for aglycone flavonoids, since these acylation sites exist only on the A, B, and C rings of the flavonoid structure [9,10]. DHM contains six active hydroxyl groups, five of which are phenolic hydroxyl groups

and the sixth is a 3-OH group on the C ring. It has been demonstrated that the 3-OH on the C ring of DHM showed the weakest antioxidant activity, and the substitution of this hydroxyl group had little effect on the antioxidant activity of DHM in comparison [11]. Currently, there are some studies into the enzymatic acylation of DHM. One of them only synthesized acetylated DHM derivatives by catalyzing DHM acylation with Novozyme 435; however, it cannot catalyze the reaction of DHM with an acyl donor of another carbon chain length. In addition, the regioselectivity was only about 85% [11]. In another study, a lipase immobilized by polydopamine-coated magnetic iron oxide nanoparticles was used to catalyze the acylation of DHM. Although acylation took place only at the 3-OH position, catalyst synthesis was cumbersome and could only catalyze the reaction of DHM with vinyl acetate; thus, this approach cannot be widely applied [2]. The reason for the deficiency in the above research may be that the lipase and solvent system used were inappropriate. Therefore, it is necessary to find a lipase with high regioselectivity and a solvent system with an appropriate polarity to improve the regioselectivity of the reaction and to synthesize DHM derivatives with different carbon chain substitutions for the exploration of biological activity.

    Thus, this study aimed to find a more suitable lipase and solvent system to improve DHM conversion and regioselectivity. The effects of several factors (i.e., the substrate molar ratio, lipase dosage, temperature, stirrer speed, reaction time, and acyl donor) on the DHM conversion, reaction rate, and regioselectivity were investigated. Subsequently, the structures of the DHM acylation derivatives were characterized by HPLC, LC-MS, and NMR spectroscopy. In addition, the liposolubility and antioxidant activities of the DHM derivatives bearing different carbon chain lengths were investigated.

2. Materials and Methods

2.1. Materials

    DHM (purity > 98%) was purchased from Bomei Biotechnology Ltd. (Hefei, Anhui, China). Soybean lecithin, methyl *tert*-butyl ether (MTBE), trichloroacetic acid (TCA), thiobarbituric acid (TBA), *tert*-butylhydroquinone (TBHQ), and vinyl acetate were purchased from Sinopharm Chemical Reagent Co., Ltd. (Shanghai, China). Vinyl butyrate, vinyl hexanoate, vinyl octanoate, and vinyl laurate were obtained from Tokyo Chemical Industry Ltd. (Tokyo, Japan). Novozyme 435 (lipase from *Candida antarctica B*), Lipozyme RM (lipase from *Rhizomucor miehei*), and Lipozyme TL IM (lipase from *Thermomyces lanuginosus*) were purchased from Novozyme Biotechnology Ltd. (Bagsvaerd, Denmark). Lipase G "Amano" 50 (lipase from *Penicillium camemberti*), Lipase AY "Amano" 30 SD (lipase from *Candida cylindracea*), Lipase AY "Amano" 400 SD (lipase from *Candida cylindracea*), Lipase MER "Amano" (lipase from *Aspergillus oryzae*), and Lipase DF "Amano" 15 (lipase from *Rhizomucor miehei*) were obtained from Amano Enzyme, Inc. (Nagoya, Aichi, Japan).

2.2. Enzymatic Acylation of DHM

    The acylation reaction was carried out in accordance with the method described by Li et al. [11], with some modification. DHM (0.18 mmol), Lipozyme TL IM, and the acyl donor were added to the solvent. The reaction was performed using a heating magnetic stirrer (IKA, Staufen, Germany). Samples were diluted 100 times with methyl alcohol and analyzed by HPLC.

2.3. Procedure for HPLC Analysis

    The acylation reactions of DHM were analyzed using an Agilent 1260 HPLC system (Santa Clara, CA, USA) equipped with an Agilent ZORBAX column (250 × 4.6 mm i.d., 5 µm) at 290 nm. The column temperature was 40 °C, injection volume was 10 µL, and flow rate was 1.0 mL/min. Mobile phase A contained acetonitrile/water/acetic acid (10/90/0.1, *v/v/v*) and mobile phase B was composed of acetonitrile/water/acetic acid (90/10/0.1, *v/v/v*). The gradient elution procedure was as follows: 0–20 min, 40–80% B; 20–25 min, 80–100% B; 25–28 min, 100–40% B; and 28–35 min, 40% B. The conversion of DHM was

calculated according to the method of Zhu et al. [12]. Additionally, the calculation formulas of the conversion and initial rate were as follows:

$$\text{Conversion (\%)} = \left(1 - \frac{A_1}{A_0}\right) \times 100 \tag{1}$$

$$V_0 = \frac{C \times n}{V \times t \times 100} \tag{2}$$

where A_0 is the amount of DHM in the initial reaction solution, A_1 is the residual amount of DHM in solution, V_0 is the initial DHM reaction rate (mmol/L·h), C is the DHM conversion in time t (%), n is the amount of DHM before the reaction (mmol), and V is the reaction system volume.

2.4. Purification of DHM Derivatives

Acylation reaction mixtures were purified using a Waters 2545 prep-HPLC equipped with a Waters XBridge Prep C18 column (250 × 19 mm i.d., 10 μm) at a detection wavelength of 290 nm. Mobile phase A was composed of methanol/water/acetic acid (10/90/0.5, *v/v/v*) and mobile phase B consisted of methanol/water/acetic acid (90/10/0.5, *v/v/v*). The gradient elution procedure was as follows: 0–20 min and 40–80% B; 20–30 min, 80–100% B; 30–35 min, 100% B; 35–37 min, 100–40% B; and 37–45 min, 40% B. The flow rate was 10 mL/min. The fractions were collected, vacuum concentrated, lyophilized, and subjected to structural identification.

2.5. Structural Identification of DHM Derivatives

The individual DHM derivatives were analyzed on a Waters BEH C18 column (150 × 2.1 mm i.d., 1.7 μm) with a flow rate of 0.3 mL/min using a Waters Synapt HDMS system (Waters, Milford, MA, USA). The detection wavelength was 290 nm, and the column temperature was 45 °C. Mobile phase A was acetonitrile, and mobile phase B consisted of formic acid/water (0.01/99.9, *v/v*). The gradient elution procedure was as follows: 0–3 min, 5–20% A; 3–6 min, 20–40% A; 6–8 min, 40–60% A; 8–10 min, 60–100% A; 10–12 min, 100% A; 12–15 min, 100–5% A. The MS conditions were set as follows: electrospray ionization negative ion (ESI⁻) mode; capillary voltage, 3000 V; cone hole voltage, 30 V; ion source temperature, 100 °C; and mass range, 50–1500 *m/z*.

Then, the specific acylation sites of DHM derivatives were further identified by a Bruker Avance III 400-MHz NMR spectrometer (Karlsruhe, Germany). The purified DHM products were dissolved in deuterated methanol (CD$_3$OD), and their ^{13}C-NMR and ^{1}H-NMR spectra were analyzed at 101 MHz and 400 MHz, respectively.

2.6. Optimization of Reaction Conditions

To optimize the reaction conditions, eight lipases, eight solvents, and five acyl donors were investigated. The effects of the reaction conditions were also assessed, including the molar ratio of DHM to vinyl butyrate (1:5–1:25), the lipase dosage (0.2–0.6 U/mg DHM), the reaction temperature (40–60 °C), the stirrer speed (0–400 rpm), and the reaction time (6–84 h). In addition to acyl donor optimization, the acyl donor in the optimization experiments was vinyl butyrate.

2.7. Determination of Octanol–Water Partition Coefficient (Log P)

DHM was reacted with fatty acid vinyl esters of various carbon chain lengths; the main DHM derivatives (3-*O*-acyl-DHM) that were acylated with vinyl acetate (C2), vinyl butyrate (C4), vinyl hexanoate (C6), vinyl octanoate (C8), and vinyl laurate (C12) were referred to as C2-DHM, C4-DHM, C6-DHM, C8-DHM, and C12-DHM, respectively. These derivatives were used in the following experiments.

The log *p* value represents the partition ratio of a substance in water and *n*-octanol. The larger the log *p* value is, the greater the liposolubility of the substance is. The method employed herein to determine the log *p* values of the various DHM derivatives was based

on that reported by Wang et al. [13]. Same volume of water and *n*-octanol were mixed, and then the mixture was poured into a liquid funnel after shaking for 24 h at 100 rpm and 30 °C, maintained for 24 h. The upper layer was water-saturated *n*-octanol, and the lower layer was *n*-octanol-saturated water. The sample (2 mg) was then dissolved in the water-saturated *n*-octanol solution (4 mL) and analyzed by HPLC. The same volume of the water-saturated *n*-octanol solution containing the sample and the *n*-octanol-saturated water solution were mixed and then shaken 24 h at 30 °C and 150 rpm. The resulting upper solution was analyzed by HPLC.

2.8. Inhibition of Lecithin Peroxidation

The inhibition effect was determined using a method previously reported by Mavi et al. [14], with some modifications. The lecithin liposome solution (0.5 mL) was added to centrifugal tubes. Then, the ferric chloride solution (3 mmol/L), ascorbic acid solution (400 μmol/L), and samples' solution were added in a final volume of 2.0 mL. The mixtures were incubated in the dark for 60 min at 37 °C. Subsequently, 1.0 mL of aqueous solution containing 0.375% (*w/v*) TBA, 15% (*w/v*) TCA, and 2.1% (*v/v*) HCl was added. The mixtures were incubated in a boiling water bath for 15 min and quickly cooled. Following centrifugation at 3500 rpm for 10 min, the supernatant liquid was collected, and its absorbance (A_1) was measured at 535 nm. Absolute ethanol was used to replace the sample in a blank tube (A_0), and the operation method was the same as that of the sample.

$$\text{Inhibition rate } (\%) = \frac{A_0 - A_1}{A_0} \times 100 \tag{3}$$

2.9. Statistical Analysis

All experimental data were collected in triplicate and analyzed independently; the results are presented as mean ± standard deviation. The results were analyzed using Origin 2018 (OriginLab Corp., Northampton, MA, USA) and IBM SPSS Statistics 22 (IBM Corp., Armonk, NY, USA); the statistical significance threshold was set to $p < 0.05$.

3. Results and Discussion

3.1. Structural Identification of DHM Derivatives

The reaction mixture of DHM and vinyl butyrate was separated and prepared by prep-HPLC, the chromatographic peaks of the three substances were obtained, as shown in Figure 1. Through the analysis of the DHM standard, peak A was the unreacted DHM and peak B and peak C were DHM acylation products, which were named as product 1 and product 2. The mass spectra of DHM and its derivatives acquired by LC-MS are displayed in Figure 2, wherein the molecular and fragment ion peaks were obtained in the negative ion mode. The peak at *m/z* 319.1 was the molecular ion peak [M-H]$^-$ of DHM; the molecular ion peak [M-H]$^-$ at *m/z* 389.1 in the mass spectrum of products revealed that one hydroxyl group of DHM was substituted by a butyryl group (molecular weight was 71). Therefore, mass spectrometry further confirmed that both products 1 and 2 were monosubstituted DHM butylated derivatives.

The acylation sites of products 1 and 2 were then determined by NMR spectroscopic analysis. For product 1, the chemical shift of C-7 moved $\triangle\delta$ 0.15 in the ^{13}C spectrum, while C-6 and C-8 also exhibited small shifts ($\triangle\delta$ 0.02) toward the high field. In terms of the ^{1}H spectrum, the changes of chemical shifts of C6-H and C8-H were $\triangle\delta$ 0.01 and $\triangle\delta$ 0.02, respectively, while the chemical shifts of other hydrogen atoms did not change, thereby confirming that the acylation substitution of product 1 occurred at 7-OH. Therefore, the structure of product 1 was identified as 7-*O*-butyryl-DHM (Figure 3A). For product 2, significant shifts of C-2 and C-4 were observed in the ^{13}C spectrum, i.e., $\triangle\delta$ 2.41 and $\triangle\delta$ 4.90, respectively, and no apparent shifts were observed for the other carbon atoms. In terms of the ^{1}H spectrum, the chemical shifts of C2-H and C3-H were moved $\triangle\delta$ 0.63 and $\triangle\delta$ 0.67, respectively, while there was no significant change in the chemical shifts of

the other hydrogen atoms ($\triangle\delta \leq 0.05$). These results indicated that product 2 exhibited acylation at the 3-OH position. Thus, the structure of product 2 was identified as 3-*O*-butyryl-DHM (Figure 3B).

The NMR data for butyryl DHM product 1 are as follows: ^{1}H NMR (400 MHz, CD$_3$OD) δ 6.55 (s, 2H, C2′-H, C6′-H), 5.91 (d, *J* = 1.9 Hz, 1H, C6-H), 5.95 (d, *J* = 1.9 Hz, 1H, C8-H), 4.86 (d, *J* = 11.4 Hz, 1H, C2-H), 4.49 (d, *J* = 11.4 Hz, 1H, C3-H), 2.32 (t, *J* = 7.3 Hz, 2H, C2″-H), 1.65 (m, *J* = 7.4 Hz, 2H, C3″-H), and 0.96 (t, *J* = 7.4 Hz, 3H, C4″-H); ^{13}C NMR (101 MHz, CD$_3$OD) δ 198.27 (C-4), 175.85(C-1″), 168.78 (C-7), 165.24 (C-5), 164.38 (C-9), 146.81 (C-3′, C-5′), 134.83 (C-4′), 129.12 (C-1′), 107.96 (C-2′, C-6′), 101.71 (C-10), 97.25 (C-6), 96.22 (C-8), 85.22 (C-2), 73.61 (C-3), 36.61 (C-2″), 19.34 (C-3″), and 13.82 (C-4″).

The NMR data for butyryl DHM product 2 are as follows: ^{1}H NMR (400 MHz, CD$_3$OD) δ 6.50 (s, 2H, C2′-H, C6′-H), 5.94 (d, *J* = 1.9 Hz, 1H, C6-H), 5.95 (d, *J* = 1.9 Hz, 1H, C8-H), 5.49 (d, *J* = 11.7 Hz, 1H, C2-H), 5.16 (d, *J* = 11.7 Hz, 1H, C3-H), 2.28 (td, *J* = 7.2, 2.5 Hz, 2H, C2″-H), 1.53 (m, *J* = 7.3, 1.4 Hz, 2H, C3″-H), and 0.81 (t, *J* = 7.4 Hz, 3H, C4″-H); ^{13}C NMR (101 MHz, CD$_3$OD) δ 193.35 (C-4), 173.52 (C-1″), 168.93 (C-7), 165.35 (C-5), 164.19 (C-9), 146.92 (C-3′, C-5′), 135.20 (C-4′), 127.63 (C-1′), 107.77 (C-2′, C-6′), 102.06 (C-10), 97.59 (C-6), 96.53 (C-8), 82.81 (C-2), 73.57 (C-3), 36.52 (C-2″), 19.37 (C-3″), and 3.58 (C-4″).
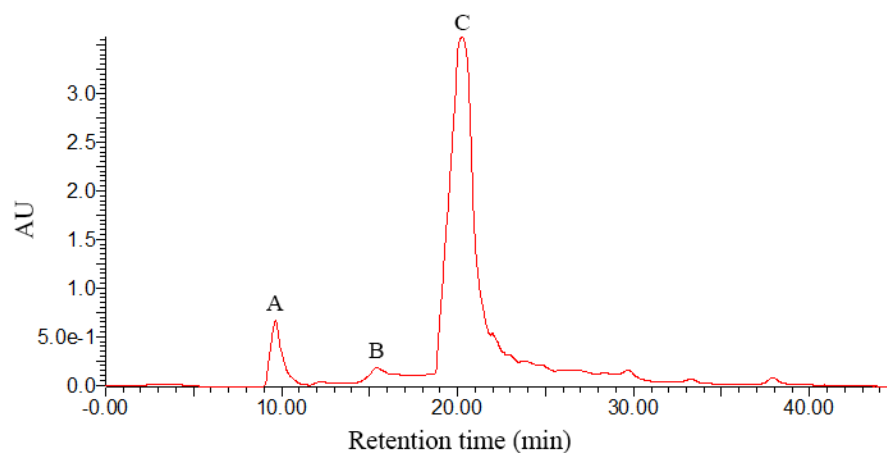

Figure 1. Prep-HPLC diagram of butyryl-DHM: (**A**) DHM; (**B**) product 1; (**C**) product 2.
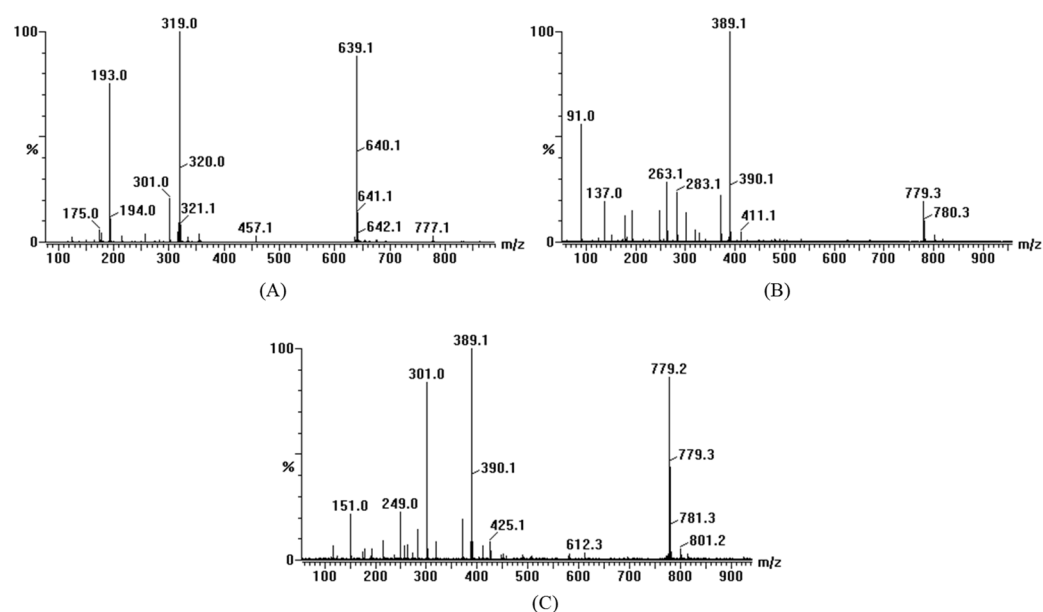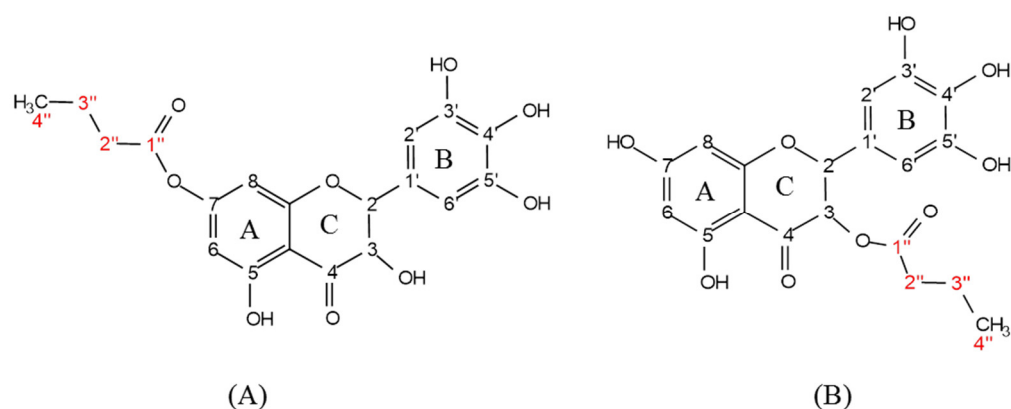

Figure 2. LC-MS spectrogram: (**A**) DHM; (**B**) product 1; (**C**) product 2.

Figure 3. Structures of the DHM acylation products: (**A**) 7-*O*-butyryl-DHM and (**B**) 3-*O*-butyryl-DHM.

3.2. Effects of Lipase

Three types of immobilized lipases and five types of free lipases were selected for optimization purposes. As illustrated in Figure 4A, when the three immobilized lipases were employed to catalyze the reaction, two products were formed. In contrast, when the five free lipases were used as catalysts, no products were formed. The highest conversion and initial reaction rate were obtained for the reaction catalyzed by Lipozyme TL IM, reaching 81.89% and 1.18 mmol/L·h, respectively, while conversions of only 5.66% and 3.79% were obtained when the reaction was catalyzed by Novozyme 435 and Lipozyme RM, respectively. These results indicated that the use of lipases of different natures and origins considerably affected the conversion and reaction rate of the acylation reaction, wherein the catalytic effects of the immobilized lipases were superior to those of the free lipases. It is possible that the thermal stabilities and the solvent stabilities of the lipases are improved by immobilization [15]. Moreover, although two products were obtained for the acylation reactions carried out using three immobilized lipases, the reaction regioselectivity differed significantly, with 3-*O*-butyryl-DHM being formed in proportions of 94.27%, 22.53%, and 10.97%, when Lipozyme TL IM, Lipozyme RM, and Novozyme 435 were used as the catalysts, respectively. Similarly, when Saik et al. [6] catalyzed quercetin acylation with lipase CAL-B and lipase PCL-C, respectively, the yield of acylation products also showed a different trend. This difference was considered to be caused by different catalytic sites of the lipase itself and the stereochemistry between the substrate and the lipase [16]. Subsequent experiments were therefore performed using Lipozyme TL IM because it afforded the highest product yield.

3.3. Effect of Solvent System

The solvent system plays a critical role in enzyme-catalyzed esterification and acylation processes. In an acylation reaction, the solvent system must impart a suitable solubility on the polar flavonoid substrates and the non-polar acyl donors, in addition to maintaining the activity of the lipase. As previously reported, solvents with different polarity had different effects on the substrate conversion, the specific binding sites between the enzyme and the substrate, and the enzyme stability [17]. Log *p* value is usually used to represent the polarity of solvents, which is the logarithm of the partition coefficient of an organic solvent in an octanol–water biphasic system [18]. Thus, we examined eight solvents with log *p* values ranging from −0.33 to 3.5. As illustrated in Figure 4B, the acylation reaction of DHM occurred in only six solvents, and the highest conversion and initial reaction rate were obtained in MTBE. More specifically, the order of conversion was as follows: MTBE (81.89%) > acetonitrile (17.38%) > 2-methyl-2-butanol (15.11%) > toluene (7.12%) > *n*-hexane (5.17%) > THF (4.76%). Laane et al. [19] classified solvents with log *p* values < 2 as polar solvents. The organic solvent with high polarity had strong hydrophilicity, which enabled them to deprive the necessary water layer on the lipase surface, thereby reducing the lipase catalytic activity [20]. Moreover, polar solvents could interact with the active sites of lipases

and destroyed the hydrogen bonds between the amino acid residues; these hydrogen bonds were vital for lipase activity [21]. However, in nonpolar solvents, the polar substrate was poorly soluble and a heterogeneous system was formed, thereby hindering the reaction [22]. The polarity of MTBE was the lowest among the six polar solvents examined herein (Figure 4C), which was less destructive to the essential water layer surrounding the lipase. Moreover, the better solubility of DHM and vinyl butyrate in this solvent was favorable for the reaction, thereby leading to the highest conversion, as mentioned above. In addition, the regioselectivity of the reaction was also found to differ in the various solvent systems examined, which was considered to be due to the different catalytic sites present in the lipase structure under different solvents. Some researchers also reported that the use of different solvents led to slight differences in the Gibbs activation energy of reaction processes, which could ultimately allow them to proceed through different routes or not at all [23,24]. Based on the above results, MTBE was the optimal solvent for the acylation reaction of DHM.
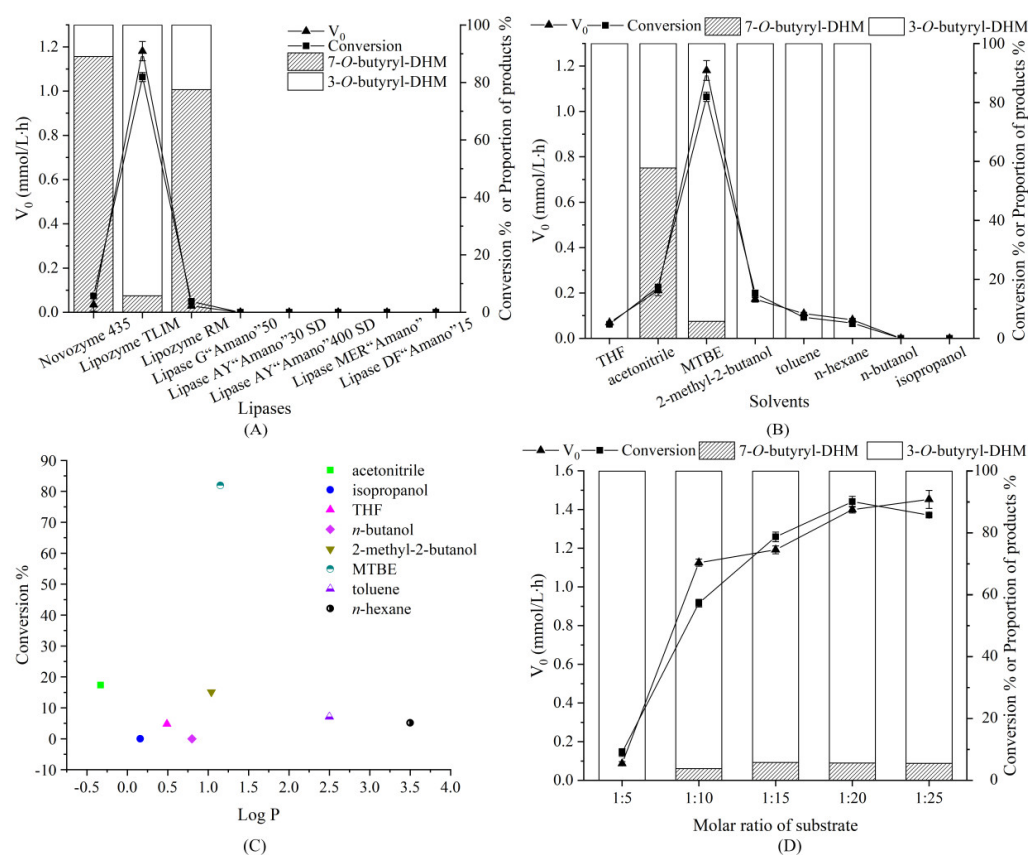
Figure 4. (**A**) Effect of lipase. Reaction conditions: DHM = 0.18 mmol, 50 °C, 200 rpm, MTBE = 10 mL, vinyl butyrate = 2.7 mmol (molar ratio of DHM to vinyl butyrate = 1:15), lipase = 0.4 U/mg DHM, time = 24 h. (**B**) Effect of the solvent system. Reaction conditions: DHM = 0.18 mmol, 50 °C, 200 rpm, Lipozyme TL IM = 0.4 U/mg DHM, vinyl butyrate = 2.7 mmol (molar ratio of DHM to vinyl butyrate = 1:15), solvent volume = 10 mL, time = 24 h. (**C**) Relationship between the log *p* value of eight solvent systems and conversion of DHM at 24 h. (**D**) Effect of molar ratio of substrate. Reaction conditions: DHM = 0.18 mmol, Lipozyme TL IM = 0.4 U/mg DHM, 50 °C, 200 rpm, MTBE = 10 mL, time = 24 h.

3.4. Effect of Substrate Molar Ratio

In acylation reactions, the molar concentration of the acyl donor is a crucial factor that influences the DHM conversion. Thus, the effects of five molar ratios of DHM to vinyl butyrate on the conversion and regioselectivity were investigated. As illustrated in Figure 4D, when the molar ratio of DHM to vinyl butyrate was increased from 1:5 to 1:20,

the conversion and initial reaction rate increased gradually and the highest conversion (i.e., 90.05%) was achieved with a 1:20 molar ratio. Therefore, the increase in the vinyl butyrate concentration facilitated the synthesis of DHM acylation products [6]. Upon increasing the molar ratio further from 1:20 to 1:25, the initial reaction rate remained constant, while the conversion decreased. This was attributed to the fact that the presence of excess vinyl butyrate could lead to lipase saturation or destruction of the lipase structure, ultimately resulting in lipase inactivation. In addition, the substrate molar ratio was found to influence the reaction's regioselectivity. When the molar ratio of the substrate was 1:5, only 3-*O*-butyryl-DHM was formed. With an increase in the substrate molar ratio to 1:15, the proportion of 3-*O*-butyryl-DHM decreased from 100% to 94.22%. Additionally, when the molar ratio of the substrate was further increased to 1:25, there was no obvious change in regioselectivity. Increasing the molar concentration of vinyl butyrate may enhance the hydrophobicity of the medium and thereby alter the reaction regioselectivity [25].
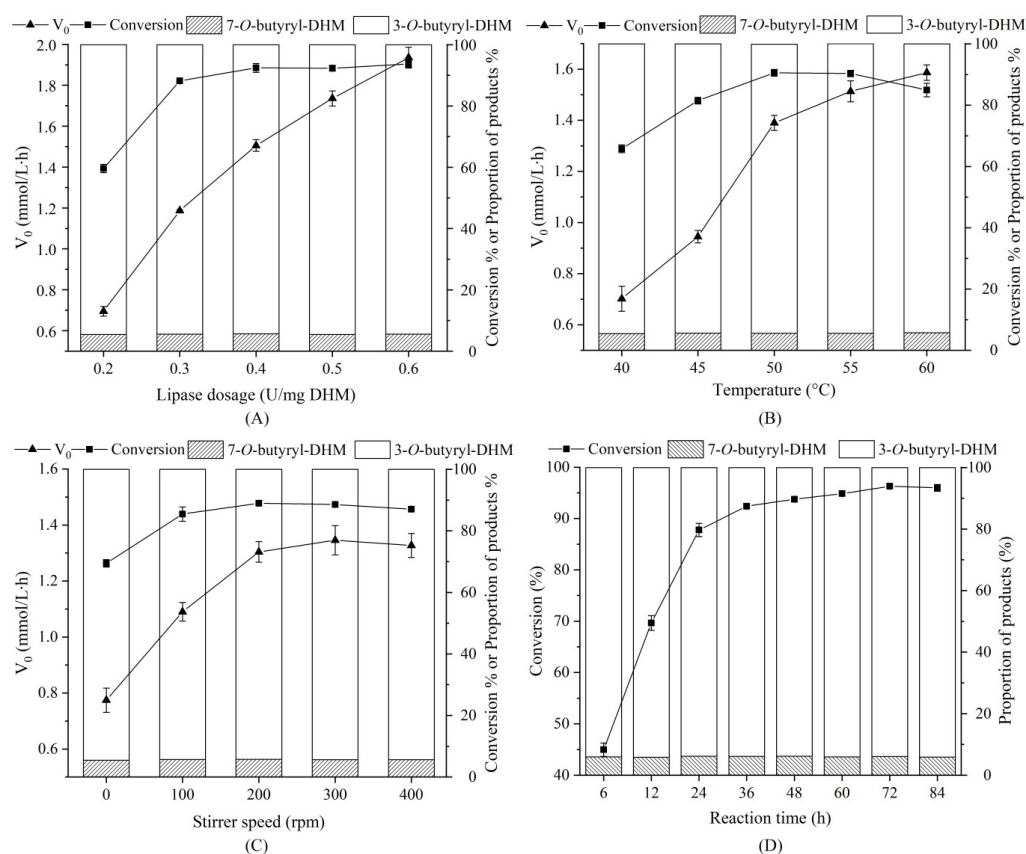
3.5. Effect of Lipase Dosage

The lipase dosage would affect the reaction rate and conversion of the acylation reaction, wherein too much or too little lipase is not conducive to the reaction. Thus, to select an appropriate lipase dosage, five dosages ranging from 0.2 to 0.6 U/mg DHM were selected, as outlined in Figure 5A. More specifically, when the lipase dosage was 0.2 U/mg DHM, the initial reaction rate and conversion were 0.69 mmol/L·h and 59.53%, respectively. When the lipase dosage increased to 0.4 U/mg DHM, the initial reaction rate and conversion reached 1.51 mmol/L·h and 92.33%, respectively, which indicated that an increase in the enzyme dosage effectively increased the contact area between the lipase and substrate. However, when the amount of the lipase was further increased to 0.6 U/mg DHM, the initial reaction rate continued to increase but the conversion tended to be stable. This was attributed to the fact that the lipase reached a saturated state; therefore, increasing the amount of the lipase did not improve the conversion. Indeed, it was possible that an increase in the lipase dosage would reduce the conversion because of mass transfer competition [26]. Additionally, a study reported that a substantial amount of the lipase addition caused waste and the immobilized lipase underwent aggregation, thereby affecting substrate diffusion [15]. In addition, when the lipase dosage was increased from 0.2 U/mg DHM to 0.6 U/mg DHM, no significant difference in the reaction's regioselectivity was observed. This result was inconsistent with that of Zhu et al. [22], but this could be due to the different enzymes and substrates used in the two studies.

3.6. Effects of Reaction Temperature, Stirrer Speed, and Reaction Time

Each lipase has an optimum temperature for its catalytic activity; therefore, five temperatures ranging from 40 to 60 °C were selected for optimization purposes. As can be seen from Figure 5B, the initial reaction rate increased from 0.70 to 1.58 mmol/L·h when the temperature was increased from 40 to 60 °C. However, the conversion increased firstly and then decreased, and the highest conversion of 90.49% was obtained at 50 °C. This suggested that upon increasing the temperature, the substrate solubility, mass transfer rate, and DHM conversion increased. Wang et al. [27] found that the catalytic activity of lipase could be improved by increasing the temperature of the microwave-assisted lipase acylation of resveratrol; however, the lipase was easily denatured and inactivated at a high temperature [28]. In addition, when the temperature is too high, the volatilization of certain solvents and substrates may affect the reaction. Moreover, Lue et al. [29] suggested that the residual water content in a system also decreased with an increase in the temperature, thereby destroying the reaction equilibrium. In addition, a negligible effect on the reaction's regioselectivity was observed over a temperature range of 40–60 °C.

Due to the fact that DHM did not fully dissolve immediately in MTBE, stirring was required to obtain a homogenous mixture and promote the reaction. As illustrated in Figure 5C, when the stirrer speed was increased from 0 to 200 rpm, both the conversion and the initial reaction rate increased, thereby demonstrating that a higher stirrer speed

can enhance contact between the lipase and the substrate to increase the mass transfer rate and conversion. However, the conversion dropped when the stirrer speed was increased from 200 to 400 rpm, which may be due to the lipase particles adhering to the wall at high stirrer speeds, thereby reducing the enzyme availability [26]. It was also possible that a high stirrer speed may destroy the structure of the lipase and reduce its activity [30]. Since no significant variation in the reaction's regioselectivity was observed over the various stirrer speeds examined, subsequent experiments were conducted at 200 rpm.


Figure 5. (**A**) Effect of lipase dosage. Reaction conditions: DHM = 0.18 mmol, vinyl butyrate = 3.6 mmol (molar ratio of DHM to vinyl butyrate = 1:20), 50 °C, 200 rpm, MTBE = 10 mL, time = 24 h. (**B**) Effect of temperature. Reaction conditions: DHM = 0.18 mmol, 200 rpm, MTBE = 10 mL, vinyl butyrate = 3.6 mmol (molar ratio of DHM to vinyl butyrate = 1:20), Lipozyme TL IM = 0.4 U/mg DHM, time = 24 h. (**C**) Effect of rotational speed. Reaction conditions: DHM = 0.18 mmol, 50 °C, MTBE = 10 mL, vinyl butyrate = 3.6 mmol (molar ratio of DHM to vinyl butyrate = 1:20), Lipozyme TL IM = 0.4 U/mg DHM, time = 24 h. (**D**) Effect of the reaction time. Reaction conditions: DHM = 0.18 mmol, 50 °C, 200 rpm, MTBE = 10 mL, vinyl butyrate = 3.6 mmol (molar ratio of DHM to vinyl butyrate = 1:20), Lipozyme TL IM = 0.4 U/mg DHM.

As illustrated in Figure 5D, upon increasing the reaction time, the DHM conversion gradually increased and reached its maximum value (96.28%) at 72 h, beyond which a slight downward trend was observed. This may be due to product accumulation and the reversible nature of the reaction, which could result in deacylation taking place. In addition, the regioselectivity of the acylation reaction did not change significantly upon increasing the reaction time to 84 h; the proportion of 3-*O*-butyryl-DHM was more than 95%. We noted that this was inconsistent with the result of Li et al. [11], wherein Novozyme 435 was used to catalyze the acetylation of DHM in acetonitrile and the regioselectivity decreased with time. This was likely due to the different catalytic activities of Lipozyme TL IM and Novozyme 435.

3.7. Effect of Acyl Donor

The carbon chain length of an acyl donor is also a critical factor that affects the acylation reaction. Thus, five acyl donors with different carbon chain lengths between C2 and C12 were examined. As illustrated in Figure 6A, upon increasing the carbon chain length, the conversion increased firstly and then decreased. More specifically, the conversion of vinyl acetate was lower than that of vinyl butyrate and vinyl hexanoate at both 24 h and 72 h, respectively; similar conversions were obtained for vinyl butyrate and vinyl hexanoate at 72 h, i.e., 95.69% and 94.76%, respectively. This was related to the solubility of the acyl donor in MTBE. Due to the solvent polarity, the solubility of vinyl acetate was lower than those of vinyl butyrate and vinyl hexanoate, which therefore influenced the reaction [31]. When the carbon chain length of the fatty acid vinyl ester was increased from C6 to C12 with a reaction time of 24 h, the conversion decreased significantly, with the conversion of the reaction involving vinyl laurate reaching only 10.28%. This was due to the increased steric hindrance with an increase in the carbon chain length, resulting in the slow reaction [32]. In addition, the effect of the acyl donor was also related to the affinity of the specific lipase to the acyl donor [33]. Overall, we found that the reaction conversions were all more than 85% at 72 h of reaction.
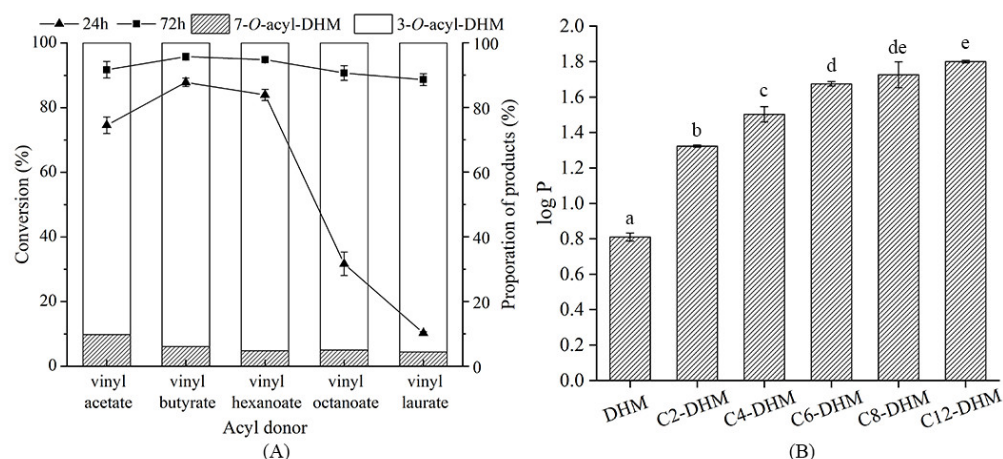
Figure 6. (**A**) Effect of the acyl donor. Reaction conditions: DHM = 0.18 mmol, 50 °C, 200 rpm, MTBE = 10 mL, acyl donor = 3.6 mmol (molar ratio of DHM to acyl donor = 1:20), Lipozyme TL IM = 0.4 U/mg DHM. (**B**) The log *p* value of DHM and its acylated derivatives (different letters indicate significant difference in the same column (*p* < 0.05)).

The carbon chain length of the acyl donor exhibited a negligible effect on the reaction's regioselectivity. More specifically, when the carbon chain length of the fatty acid vinyl ester was increased from C2 to C4, the regioselectivity increased slightly; upon increasing further to C12, no significant change was observed.

3.8. Determination of Octanol–Water Partition Coefficient (log P)

From Figure 6B, upon increasing the carbon chain length of the acyl donor, the log *p* values of the acylated derivatives of DHM gradually increased. More specifically, the log *p* values of DHM and its five derivatives (i.e., C2-DHM, C4-DHM, C6-DHM, C8-DHM, and C12-DHM) were 0.81, 1.32, 1.50, 1.67, 1.72, and 1.80, respectively, which demonstrated that an increase in the carbon chain length reduced molecule polarity while increasing lipophilicity.

3.9. Inhibition of Lecithin Peroxidation

As can be seen from Figure 7, in the lecithin peroxidation system, the inhibition ability of Vc, TBHQ, and DHM and its derivatives increased with an increase in the sample concentration. At a concentration of 1.0 mg/mL, the inhibition ability order of lecithin peroxidation was TBHQ > C8-DHM > C6-DHM > C4-DHM > C2-DHM > C12-DHM > DHM > Vc, thereby

indicating that the antioxidant activities of DHM derivatives were higher than that of DHM itself and the inhibition ability of C8-DHM was close to that of TBHQ. This can be accounted for by considering that the lipid-soluble free radicals present on lecithin that were induced by iron ion–ascorbic acid were located in the hydrophobic region of the bilayer. After DHM acylation, the liposolubility was enhanced and easily entered the hydrophobic region of the lecithin bilayer to come into contact with the lipid-soluble free radicals. In addition, the inhibition of lecithin peroxidation was gradually increased as the carbon chain length increased from C2 to C8 but it decreased significantly as the carbon chain length further increased from C8 to C12. This is consistent with the nonlinear theory (cutoff effect) proposed by previous researchers in studies into lipid oxidation and emulsion oxidation [34,35]. Furthermore, the steric hindrance associated with the longer alkyl chains may prevent long-chain esters from entering the lecithin bilayer and coming into contact with free radicals, which also account for a cutoff effect [36].
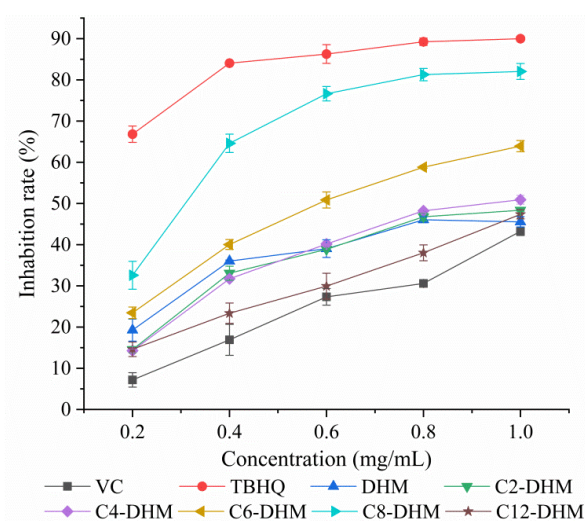

Figure 7. Inhibition ability of DHM and its derivatives on lipid peroxidation.

4. Conclusions

DHM could be acylated with acyl donors of varying carbon chain lengths, which revealed that this process was not limited only to the use of vinyl acetate. Indeed, both short- and medium-chain vinyl fatty acid esters were found to be more conducive to the reaction. Two products, namely, 7-*O*-acyl-DHM and 3-*O*-acyl-DHM, were found in this reaction. Furthermore, the liposolubility of the DHM derivatives were found to increase upon increasing the length of the acyl substituent, and the antioxidant activities of the DHM derivatives were higher than that of DHM in the lecithin peroxidation system. Thus, the application of DHM in a food lipid system will be broadened by acylation. Although the antioxidant activity of the derivatives in a lecithin peroxidation system was higher than that of DHM, the reaction system was a chemical system, which cannot really reflect the antioxidant activity in a food model or biological system. In addition, only the derivatives with the most substituted carbon chain of C12 were synthesized, while the antioxidant activity of the derivatives with a longer substituted carbon chain was unknown. Therefore, it is necessary to further synthesize derivatives with longer carbon chains and study the antioxidant activity and mechanism of DHM derivatives in different reaction systems.

Institutional Review Board Statement: Not applicable.

Informed Consent Statement: Not applicable.

Data Availability Statement: All data generated or analyzed during this study are included in this manuscript.

Conflicts of Interest: The authors declare no competing financial interest.

References

1. Liu, D.; Mao, Y.Q.; Ding, L.J.; Zeng, X.A. Dihydromyricetin: A review on identification and quantification methods, biological activities, chemical stability, metabolism and approaches to enhance its bioavailability. *Trends Food Sci. Technol.* **2019**, *91*, 586–597. [CrossRef] [PubMed]
2. Cao, S.L.; Deng, X.; Xu, P.; Huang, Z.X.; Zhou, J.; Li, X.H.; Zong, M.H.; Lou, W.Y. Highly efficient enzymatic acylation of dihydromyricetin by the immobilized lipase with deep eutectic solvents as cosolvent. *J. Agric. Food Chem.* **2017**, *65*, 2084–2088. [CrossRef] [PubMed]
3. Tong, H.H.; Zhang, X.J.; Tan, L.F.; Jin, R.M.; Huang, S.L.; Li, X. Multitarget and promising role of dihydromyricetin in the treatment of metabolic diseases. *Eur. J. Pharmacol.* **2020**, *870*, 172888. [CrossRef]
4. Liu, B.G.; Du, J.Q.; Zeng, J.; Chen, C.G.; Niu, S.Y. Characterization and antioxidant activity of dihydromyricetin–lecithin complex. *Eur. Food Res. Technol.* **2009**, *230*, 325–331. [CrossRef]
5. Plaza, M.; Pozzo, T.; Liu, J.Y.; Gulshan Ara, K.Z.; Turner, C.; Karlsson, E.N. Substituent effects on in vitro antioxidizing properties, stability, and solubility in flavonoids. *J. Agricutural Food Chem.* **2014**, *62*, 3321–3333. [CrossRef] [PubMed]
6. Saik, A.Y.H.; Lim, Y.Y.; Stanslas, J.; Choo, W.S. Lipase-catalyzed acylation of quercetin with cinnamic acid. *Biocatal. Biotransform.* **2016**, *34*, 33–43. [CrossRef]
7. Chebil, L.; Antihoni, J.; Huweau, C.; Gerardin, C.; Engasser, J.M.; Ghoul, M. Enzymatic acylation of flavonoids: Effect of the nature of the substrate, origin of lipase, and operating conditions on conversion yield and regioselectivity. *J. Agric. Food Chem.* **2007**, *55*, 9496–9502. [CrossRef]
8. Yu, M.; Liu, B.; Zhong, F.; Wan, Q.; Zhu, S.; Huang, D.; Li, Y. Interactions between caffeic acid and corn starch with varying amylose content and their effects on starch digestion. *Food Hydrocoll.* **2021**, *114*, 106544. [CrossRef]
9. Chebil, L.; Humeau, C.; Falcimaigne, A.; Engasser, J.M.; Ghoul, M. Enzymatic acylation of flavonoids. *Process Biochem.* **2006**, *41*, 2237–2251. [CrossRef]
10. Dong, W.X.; Chen, D.J.; Chen, Z.Y.; Sun, H.Y.; Xu, Z.M. Antioxidant capacity differences between the major flavonoids in cherry (*Prunus pseudocerasus*) in vitro and in vivo models. *LWT Food Sci. Technol.* **2021**, *141*, 110938. [CrossRef]
11. Li, W.; Wu, H.; Liu, B.G.; Hou, X.D.; Wan, D.J.; Lou, W.Y.; Zhao, J. Highly efficient and regioselective synthesis of dihydromyricetin esters by immobilized lipase. *J. Biotechnol.* **2015**, *199*, 31–37. [CrossRef] [PubMed]
12. Zhu, S.; Meng, N.; Chen, S.W.; Li, Y. Study of acetylated EGCG synthesis by enzymatic transesterfication in orgnic media. *Arab. J. Chem.* **2020**, *13*, 8824–8834. [CrossRef]
13. Wang, S.; Li, Y.; Meng, X.Y.; Chen, S.W.; Huang, D.J.; Xia, Y.M.; Zhu, S. Antioxidant activities of chlorogenic acid derivatives with different acyl donor chain lengths and their stabilities during in vitro simulated gastrointestinal digestion. *Food Chem.* **2021**, *357*, 129904. [CrossRef] [PubMed]
14. Mavi, A.; Lawrence, G.D.; Kordali, S.; Yildirim, A.L.I. Inhibition of Iron-Fructose-Phosphate-Induced lipid peroxidation in lecithin liposome and linoleic acid emulsion systems by some edible plants. *J. Food Biochem.* **2011**, *35*, 833–844. [CrossRef]
15. Yadav, G.; Pawar, S.V. Synergism between microwave irradiation and enzyme catalysis in transesterification of ethyl-3-phenylpropanoate with n-butanol. *Bioresour. Technol.* **2012**, *109*, 1–6. [CrossRef]
16. Zare, M.; Golmakani, M.T.; Niakousari, M. Lipase synthesis of isoamyl acetate using different acyl donors: Comparison of novel esterification techniques. *LWT Food Sci. Technol.* **2019**, *101*, 214–219. [CrossRef]
17. Hazarika, S.; Goswami, P.; Dutta, N.N. Lipase catalysed transesterification of 2-O-benzylglycerol with vinyl acetate: Solvent effect. *Chem. Eng. J.* **2003**, *94*, 1–10. [CrossRef]
18. Lu, J.; Nie, K.; Wang, F.; Tan, T.W. Immobilized lipase *Candida* sp. 99–125 catalyzed methanolysis of glycerol trioleate: Solvent effect. *Bioresour. Technol.* **2008**, *99*, 6070–6074. [CrossRef]
19. Laane, C.; Boeren, S.; Vos, K.; Veeger, C. Rules for optimization of biocatalysis in organic solvents. *Biotechnol. Bioeng.* **1987**, *30*, 81–87. [CrossRef]

20. Yadav, G.; Hude, M.P.; Talpade, A.D. Microwave assisted process intensification of lipase catalyzed transesterification of 1,2 propanediol with dimethyl carbonate for the green synthesis of propylene carbonate: Novelties of kinetics and mechanism of consecutive reactions. *Chem. Eng. J.* **2015**, *281*, 199–208. [CrossRef]

21. Jahangiri, A.; Moller, A.H.; Danielsen, M.; Madsen, B.; Joernsgaard, B.; Vaerbak, S.; Adlercreutz, P.; Dalsgaard, T.K. Hydrophiliza-tion of bixin by lipase-catalyzed transesterification with sorbitol. *Food Chem.* **2018**, *268*, 203–209. [CrossRef] [PubMed]

22. Zhu, S.; Wang, S.; Chen, S.W.; Xia, Y.M.; Li, Y. Lipase-catalyzed highly regioselective synthesis of acylated chlorogenic acid. *Food Biosci.* **2020**, *37*, 100706. [CrossRef]

23. Cao, Z.D.; Zhang, R.K.; Hu, X.R.; Sha, J.; Jiang, G.L.; Li, Y.; Li, T.; Ren, B.Z. Thermodynamic modelling, Hansen solubility parameter and solvent effect of oxaprozin in thirteen pure solvents at different temperatures. *J. Chem. Thermodyn.* **2020**, *151*, 106239. [CrossRef]

24. Zheng, M.; Chen, J.; Chen, G.Q.; Farajtabar, A.; Zhao, H. Solubility modelling and solvent effect for domperidone in twelve green solvents. *J. Mol. Liq.* **2018**, *261*, 50–56. [CrossRef]

25. Lorentz, C.; Dulac, A.; Pencreac'h, G.; Ergan, F.; Richomme, P.; Soultani-Vigneron, S. Lipase-catalyzed synthesis of two new antioxidants: 4-*O*- and 3-*O*-palmitoyl chlorogenic acids. *Biotechnol. Lett.* **2010**, *32*, 1955–1960. [CrossRef]

26. Bhavsar, K.V.; Yadav, G.D. Process intensification by microwave irradiation in immobilized-lipase catalysis in solvent-free synthesis of ethyl valerate. *Mol. Catal.* **2018**, *461*, 34–39. [CrossRef]

27. Wang, Z.; Zhang, Y.X.; Zheng, L.; Cui, X.Y.; Huang, H.; Geng, X.; Xie, X.N. Regioselective acylation of resveratrol catalyzed by lipase under microwave. *Green Chem. Lett. Rev.* **2018**, *11*, 312–317. [CrossRef]

28. Ziaullah, K.S.; Rupasinghe, H.P. Sonochemical enzyme-catalyzed regioselective acylation of flavonoid glycosides. *Bioorgnic Chem.* **2016**, *65*, 17–25. [CrossRef]

29. Lue, B.M.; Guo, Z.; Xu, X.B. Effect of room temperature ionic liquid structure on the enzymatic acylation of flavonoids. *Process Biochem.* **2010**, *45*, 1375–1382. [CrossRef]

30. De Souza, R.O.; Antunes, O.A.; Kroutil, W.; Kappe, C.O. Kinetic resolution of rac-1-phenylethanol with immobilized lipases: A critical comparison of microwave and conventional heating protocols. *J. Org. Chem.* **2009**, *74*, 6157–6162. [CrossRef]

31. Ardhaoui, M.; Falcimaigne, A.; Ognier, S.; Engasser, J.M.; Moussou, P.; Pauly, G.; Ghoul, M. Effect of acyl donor chain length and substitutions pattern on the enzymatic acylation of flavonoids. *J. Biotechnol.* **2004**, *110*, 265–271. [CrossRef] [PubMed]

32. Deng, X.; Cao, S.L.; LI, N.; Wu, H.; Smith, T.J.; Zong, M.H.; Lou, W.Y. A magnetic biocatalyst based on mussel-inspired polydopamine and its acylation of dihydromyricetin. *Chin. J. Catal.* **2016**, *37*, 584–595. [CrossRef]

33. Enaud, E.; Humeau, C.; Piffaut, B.; Girardin, M. Enzymatic synthesis of new aromatic esters of phloridzin. *J. Mol. Catal. B Enzym.* **2004**, *27*, 1–6. [CrossRef]

34. Bayrasy, C.; Chabi, B.; Laguerre, M.; Lecomte, J.; Jublanc, E.; Villeneuve, P.; Wrutniak-Cabello, C.; Cabello, G. Boosting antioxidants by lipophilization: A strategy to increase cell uptake and target mitochondria. *Pharm. Res.* **2013**, *30*, 1979–1989. [CrossRef] [PubMed]

35. Oh, W.Y.; Shahidi, F. Antioxidant activity of resveratrol ester derivatives in food and biological model systems. *Food Chem.* **2018**, *261*, 267–273. [CrossRef]

36. Laguerre, M.; Lopez Giraldo, L.J.; Lecomte, J.; Figueroa-Espinoza, M.C.; Barea, B.; Weiss, J.; Decker, E.A.; Villeneuve, P. Relationship between hydrophobicity and antioxidant ability of "phenolipids" in emulsion: A parabolic effect of the chain length of rosmarinate esters. *J. Agricultural Food Chem.* **2010**, *58*, 2869–2876. [CrossRef]